PROGRESS IN MULTIRATE AND TURBULENCE MODELING

E. Itam[(1)], B. Koobus[(1)]

(1) IMAG, Université de Montpellier, France.

MAIDESC meeting - May 2017

Introduction

Work context

- Implementation and development of a simulation tool whose major ingredients are :
  - A numerical model suited to **industrial problems**
    - Ongoing investigation : **multirate schemes**
  - Turbulence models suited to the simulation of **turbulent flows** with massive separation and vortex shedding, for a large range of Reynolds numbers
    - Ongoing investigation : **hybrid RANS/VMS-LES models**

Turbulence modelling

In the present work

- Evaluation of hybrid turbulence models (DDES and RANS/VMS-LES) for the prediction of the flow around a **circular cylinder** in **subcritical regimes** :
  - Test cases that contain many features and difficulties encountered in industrial problems
  - Well documented benchmarks
  - First step before the computation of array of cylinders (offshore oil and gas industries, civil engineering, aeronautics)
  - Good candidates to test the multirate approach (boundary layers)

Hybrid RANS/VMS-LES model

Motivations

- Computation of **massively separated flows at high Reynolds number** on unstructured mesh
- A model also applicable to **subcritical flows** (moderate Reynolds number and laminar boundary layer)
- **RANS** : accuracy problems in flow regions with massive separation (as the flow around bluff-bodies)
- **VMS-LES** : more expensive than RANS, very fine resolution requirements in boundary layers at high Reynolds number
- **Hybrid : combines RANS and VMS-LES** in order to exploit the advantages of the two approaches :
  - **less computationally** expensive compared with VMS-LES
  - **better accuracy** than RANS for flows dominated by large unsteady structures
- Desired features for the hybridation strategy : **automatic and progressive switch** from RANS to VMS-LES and vice versa + **automatic RANS shielding zone**

Hybrid RANS/VMS-LES model

- **Central idea of the proposed hybrid VMS model** :
  Correction of the mean flow field obtained with a RANS model by adding fluctuations given by a VMS-LES approach wherever the grid resolution is adequate

- **Decomposition of the flow variables** :

$$W = \underbrace{< W >}_{RANS} + \underbrace{W^c}_{correction} + W^{SGS}$$

$< W >$ = RANS flow variables
W^c = remaining resolved fluctuations obtained with VMS-LES
(i.e. $< W > + W^c = W_h$ = VMS-LES flow variables)
W^{SGS} = subgrid scale fluctuations

Hybrid RANS/VMS-LES model

Hybrid RANS/VMS-LES governing equations

- **Semi-discretization of the RANS equations** ($k-\epsilon$ Goldberg model + Menter correction) :

$$\left(\frac{\partial\langle W\rangle}{\partial t},\Phi_i\right)+(\nabla\cdot F(\langle W\rangle),\Phi_i)=-\left(\tau^{RANS}(\langle W\rangle),\Phi_i\right).$$

- **Final hybrid VMS model equations** (RANS eq. + modified governing eq. for reconstructed fluctuations) :

$$\left(\frac{\partial W_h}{\partial t},\Phi_i\right)+(\nabla\cdot F(W_h),\Phi_i)=$$
$$-\theta\left(\tau^{RANS}(\langle W\rangle),\Phi_i\right)-(1-\theta)\left(\tau^{LES}(W_h'),\Phi_i'\right)$$

  where W_h denotes the hybrid variables

- $\theta\in[0,1]$ **is the blending function**

Hybrid RANS/VMS-LES model

Hybridization strategy

$$\boxed{\theta = 1 - f_d(1 - \bar{\theta})}$$

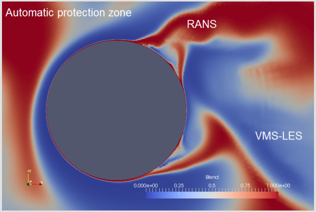

$f_d \simeq 0$ in the boundary layer
$f_d \simeq 1$ outside the boundary layer

$$\text{where } \bar{\theta} = tanh(\xi^2) \text{ with } \xi = \frac{\Delta}{l_{RANS}} \text{ or } \xi = \frac{\mu_{SGS}}{\mu_{RANS}},$$

$$f_d = 1 - tanh((8r_d)^3) \text{ and } r_d = \frac{\nu_t + \nu}{max(\sqrt{u_{i,j}u_{i,j}}, 10^{-10})K^2 d_w^2}$$

DDES

A DDES model :

- Based on the low Reynolds $k - \epsilon$ model proposed by **Goldberg**
- The turbulent viscosity is limited by the **Bradshaw's law** in a similar way to Menter's SST model

DDES/$k - \varepsilon$/Menter formulation

The dissipation term $D_k^{RANS} = \rho\varepsilon$ in the RHS of the $k - \epsilon$ equations is replaced by:

$$D_k^{DDES} = \rho \frac{k^{3/2}}{l_{DDES}}$$

with $l_{DDES} = \frac{k^{3/2}}{\epsilon} - f_d max \left(0, \frac{k^{3/2}}{\epsilon} - C_{DDES}\Delta\right)$ where $C_{DDES} = 0.65$ and Δ is a measure of local mesh size

Circular cylinder at Re $= 3900 \backsim$ Subcritical regime

Test case definition

- **Flow parameters:**
  Mach $= 0.1$
  Reynolds $= 3900$

- **Computational grid:**
  1.46M nodes
  8.4M elements

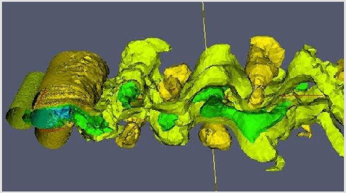

Circular cylinder at Re= 3900 $\backsim$ Subcritical regime

	$\overline{C}_d$	$-\overline{C}_{p_b}$	C_L^{rms}	L_r
Experiments				
Norberg Min	0.94	0.83	-	-
Norberg Max	1.04	0.93	-	-
Parnaudeau	-	-	-	1.51
Present simulations				
No model	0.87	0.73	0.04	2.11
RANS $k-\varepsilon$/Menter	0.86	0.72	0.03	2.18
DDES $k-\varepsilon$/Menter	0.88	0.74	0.03	2.07
DVMS	0.96	0.84	0.12	1.54
H-RANS/DVMS	0.91	0.77	0.05	1.80
Other simulations				
Wissink (DNS)				1.588
Tremblay (DNS)	1.03	0.93		
Ma (DNS)		0.93		
Froehlich (LES)	1.08	1.03		1.09
D'Alessandro SA-IDDES	0.98	0.83	0.109	1.67
D'Alessandro $\bar{v}^2-f$ DES	1.02	0.87	0.14	1.42
Malizia $k-\omega$ SST	1.04		.188	1.356
Malizia LES-Dyn-Sm	1.03		.196	1.307

Table 1: **Circular cylinder: bulk flow parameters at Re=3900**

Circular cylinder at Re $= 20 \times 10^3$ ∽ Subcritical regime

Test case definition

- **Flow parameters** :
  Reynolds $= 20 \times 10^3$
  Mach=0.1

- **Computational grid** :
  1.8M nodes
  9.4M elements

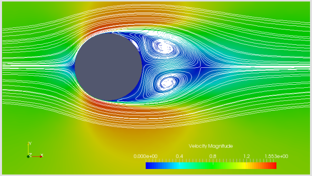

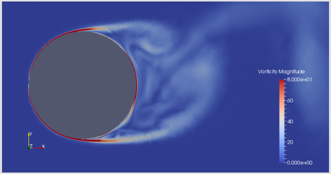

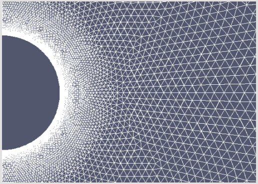

Circular cylinder at $Re = 20 \times 10^3 \backsim$ Subcritical regime

	$\overline{C_d}$	C_L^{rms}	$-\overline{Cp_b}$	Θ_{sep}	Lr
Experiments					
Norberg	1.16	0.47	1.16	78	1.03
Present simulations					
No model	1.27	0.61	1.35	82	0.96
RANS $k-\varepsilon$/Menter	1.27	0.71	1.25	85	0.64
DDES $k-\varepsilon$/Menter	1.16	0.36	1.12	82	0.83
DVMS	1.18	0.46	1.20	81	0.96
H-RANS/DVMS	1.15	0.46	1.15	86	0.88
Other simulations					
Aradag LES Min			1.04		
Aradag LES Max			1.25		
Salvatici LES Min	0.94	0.17	0.83		
Salvatici LES Max	1.28	0.65	1.38		

Table 2: **Circular cylinder : bulk flow parameters at Re=20000**

Circular cylinder at Re = 140000 ∽ Subcritical regime

	$\overline{C_d}$	C_L^{rms}	$-\overline{Cp_b}$	Θ_{sep}	Lr
Experiments					
Cantwell and Coles	1.24		1.21	77	0.5
Kim, Lee, Kim, Choi	1.27		1.36		
Present simulations					
No model	0.49	0.14	0.53	90	0.93
RANS $k-\varepsilon$/Menter	0.77	0.31	0.84	99	0.80
DDES $k-\varepsilon$/Menter	0.97	0.30	1.01	92	0.96
DVMS	1.21	0.69	1.39	81	0.98
H-RANS/DVMS	0.77	0.35	0.86	99	0.86
Other simulations					
Travin DES/SA	0.87	0.10	0.81	78	1.5
Hans-Krajnovic LES Smago Dyn	1.18		1.24	92	0.57
Breuer LES Smago	1.28		1.51	94	0.46

Table 3: **Circular cylinder : bulk flow parameters at Re=140000**

Multirate time advancing by volume agglomeration

Work context

- Development of a new **explicit multirate time advancing scheme** for the solution of the compressible Navier-Stokes equations :
  - based on control volume agglomeration
  - well suited to our numerical framework using a mixed finite volume/finite element formulation
  - developed in a parallel numerical framework

Multirate time advancing by volume agglomeration

Multirate based on agglomeration - Objectives

A frequent configuration in CFD calculations combines :

- An explicit time advancing scheme for accuracy purpose
- A computational grid with a very small portion of much smaller elements than in the remaining mesh

Examples:

- *Isolated traveling shock*
- *Boundary layer at high Reynolds number (few tens of microns thick) in LES computations where vortices around one centimeter are captured*

Explicit time advancing schemes with global time stepping are too costly
$\longrightarrow$ the **multirate time stepping approach** is an interesting alternative

Multirate time advancing by volume agglomeration

Inner and outer zones - Definition

- **Inner and outer zones** :
  - Let Δt be the global time step over the computational domain
  - Define the **outer zone** as the set of cells for which the explicit scheme is stable for a time step $K\Delta t$, and the **inner zone** as its complement
  - Definition of these zones through the local time steps

Multirate time advancing by volume agglomeration

Inner and outer zones - Definition

- **Inner and outer zones** :
  - Let Δt be the global time step over the computational domain
  - Define the **outer zone** as the set of cells for which the explicit scheme is stable for a time step $K\Delta t$, and the **inner zone** as its complement
  - Definition of these zones through the local time steps

Coarse grid

- **Objective** :
  - Advancement in time with time step $K\Delta t$
  - Advancement in time preserving accuracy in the outer zone (space order of 3, RK4)
  - Advancement in time consistent in the inner zone
- Define the **coarse grid** as the macro cells in the inner zone + the fine cells in the outer zone

Multirate time advancing by volume agglomeration

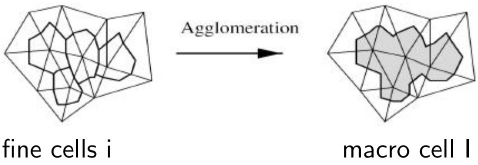

Multirate based on agglomeration - Definition

- Flux on the coarse grid :
  - Assembling of the nodal flux Ψ_i on the fine cells (as usual)
  - Fluxes sum on the macro cells I (inner zone) :

$$\Psi^I = \sum_{k \in I} \Psi_k$$

- Volumes sum on the macro cells I (inner zone) : $Vol^I = \sum_{k \in I} Vol_k$ where Vol_k is the volume of $cell_k$

Multirate time advancing by volume agglomeration

Multirate based on agglomeration - Algorithm

Step 1 (predictor on the coarse grid) :

Advancement in time with Runge-Kutta (for example) on the macro cells in the inner zone and on the fine cells in the outer zone, with time step $K\Delta t$:

For $\alpha = 1, RKstep$

$$\text{outer zone :} \quad vol_i w_i^{(\alpha)} = vol_i w_i^{(0)} + b_\alpha K\Delta t \, \Psi_i^{(\alpha-1)}$$

$$\text{inner zone :} \quad vol^I w^{I,(\alpha)} = vol^I w^{I,(0)} + b_\alpha K\Delta t \, \Psi^{I,(\alpha-1)}$$

$$w_i^{(\alpha)} = w^{I,(\alpha)} \quad \text{for } i \in I$$

EndFor α.

Multirate time advancing by volume agglomeration

Multirate based on agglomeration - Algorithm

Step 2 (corrector in the inner zone) :

- Unknowns frozen in the outer zone
- Time interpolation of these unknowns (those useful for the next point)
- In the inner zone : using these interpolated values, advancement in time with the chosen explicit scheme and time step Δt
- Complexity mastered (proportional to the number of points in the inner zone)

$$\longrightarrow \text{CostMultirate(K)} = \text{CostExplicit(N)*(1/K} + \text{Ninnernodes(K)/N)}$$

ALE calculation of a traveling contact discontinuity

Test case definition

- **Simulation** :
  - Compressible Euler equations are solved in a rectangular parallelepiped
  - Density is initially discontinuous at the middle of the domain
  - Velocity and pressure are uniform
- **A deforming mesh** :

Nodes	Elements	Subdomains
25K	92K	2

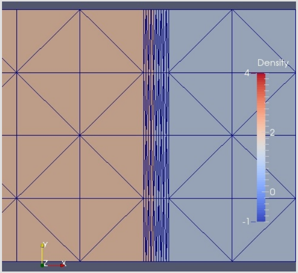

Figure 1: Instantaneous mesh with mesh concentration in the middle of zoom

ALE calculation of a traveling contact discontinuity

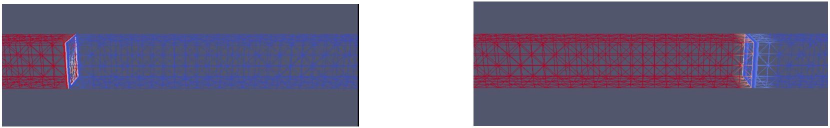

Figure 2: Zooms on the moving contact discontinuity using a load balancing procedure at two different time steps

K	CPU explicit (s/Δt/node)	$N^{small}(K)/N$ (%)	Expected gain (scalar)	CPU pred. phase (s/KΔt)	CPU correc. phase (s/KΔt)	Measured gain (parallel)
5	$4.96.10^{-6}$	1.3	4.7	0.124	0.244	1.7
10	$4.96.10^{-6}$	1.3	8.8	0.124	0.482	2.0
15	$4.96.10^{-6}$	1.3	12.5	0.124	0.729	2.2

Table 4: **ALE propagation of a contact discontinuity**: Time step factor K, CPU of the explicit scheme per explicit time-step Δt and per node, percentage of nodes in the inner region, theoretical gain in scalar mode, CPU of the prediction phase per time-step $K\Delta t$, CPU of the correction phase per time-step $K\Delta t$, and measured parallel gain.

Tandem Cylinders

Test case definition

- **Simulation** :
  Hybrid VMS-LES simulation combined with non-dynamic and dynamic versions of the WALE SGS model

- **Flow parameters** :
  Reynolds $= 1.66 \times 10^5$
  Mach=0.1
  $L/D = 3.7$

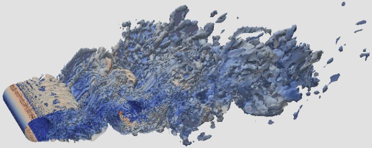

Tandem Cylinders

Test case definition

- **Simulation** :
  Hybrid VMS-LES simulation combined with non-dynamic and dynamic versions of the WALE SGS model

- **Computational grid** :

Nodes	Elements	Subdomains
16M	92M	768

- **Flow parameters** :
  Reynolds $= 1.66 \times 10^5$
  Mach=0.1
  $L/D = 3.7$

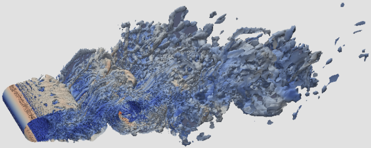

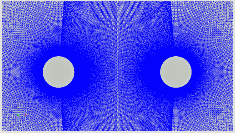

Tandem Cylinders

Figure 3: Animation of Q-criterion to observe the vortical structures in the flow

K	CPU explicit (s/Δt/node)	$N^{small}(K)/N$ (%)	Expected gain (scalar)	CPU pred. phase (s/KΔt)	CPU cor. phase (s/KΔt)	Measured gain (parallel)
5	10^{-7}	18	2.63	1.55	6.93	0.91
10	10^{-7}	24	2.94	1.52	14.15	0.99
20	10^{-7}	35	2.50	1.53	28.94	1.02

Table 5: **Tandem cylinder - fine mesh**: Time step factor K, CPU of the explicit scheme per explicit time-step Δt and per node, percentage of nodes in the inner region, theoretical gain in scalar mode, CPU of the prediction phase per time-step $K\Delta t$, CPU of the correction phase per time-step $K\Delta t$, and measured parallel gain.

Cylinder

Test case definition

- **Simulation** :
  Hybrid VMS-LES simulation combined with non-dynamic version of the WALE SGS model

- **Flow parameters** :
  Reynolds $= 8.4 \times 10^6$
  Mach$=0.1$

Cylinder

Test case definition

- **Simulation** :
  Hybrid VMS-LES simulation combined with non-dynamic version of the WALE SGS model

- **Flow parameters** :
  Reynolds $= 8.4 \times 10^6$
  Mach=0.1

- **Computational grid** :

Nodes	Elements	Subdomains
4.3M	25M	768

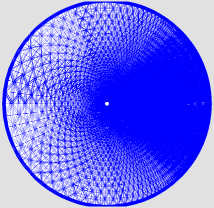

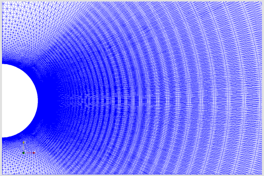

Cylinder

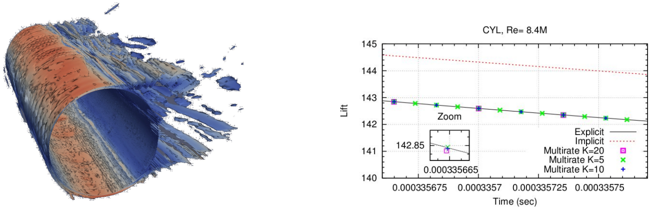

Figure 4: Left: Instantaneous Q-criterion isosurfaces; Right: Lift curves for explicit, implicit and multirate schemes.

K	CPU explicit (s/Δt/node)	$N^{small}(K)/N$ (%)	Expected gain (scalar)	CPU pred. phase (s/KΔt)	CPU cor. phase (s/KΔt)	Measured gain (parallel)	Error (%)
5	$8.4\ 10^{-8}$	15	2.86	0.39	1.53	1.02	$4.4\ 10^{-4}$
10	$8.4\ 10^{-8}$	19	3.45	0.39	3.12	1.11	$7.8\ 10^{-4}$
20	$8.4\ 10^{-8}$	24	3.45	0.39	6.24	1.18	$2.6\ 10^{-3}$
Implicit						12.12	1.0

Table 6: **Circular cylinder**: Time step factor K, CPU of the explicit scheme per explicit time-step Δt and per node, percentage of nodes in the inner region, theoretical gain in scalar mode, CPU of the prediction phase per time-step $K\Delta t$, CPU of the correction phase per time-step $K\Delta t$, measured parallel gain, and relative error.

Space probe model

Test case definition

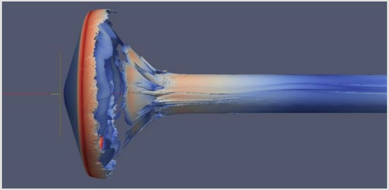

- **Flow parameters** :
  Reynolds $= 1 \times 10^6$
  Mach=2.0

- **Simulation** :
  Hybrid VMS-LES simulation combined with non-dynamic version of the WALE SGS model

Space probe model

Test case definition

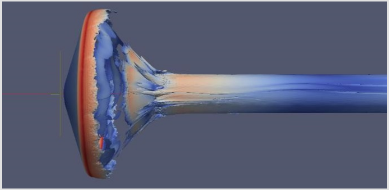

- **Flow parameters** :
  Reynolds $= 1 \times 10^6$
  Mach=2.0

- **Simulation** :
  Hybrid VMS-LES simulation combined with non-dynamic version of the WALE SGS model

- **Computational grid** :

Nodes	Elements	Subdomains
4.38M	25.8M	192

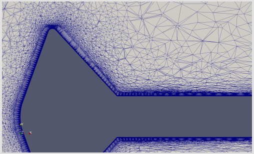

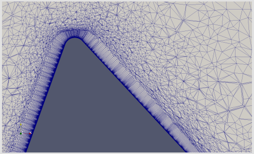

Space probe model

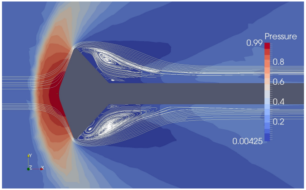

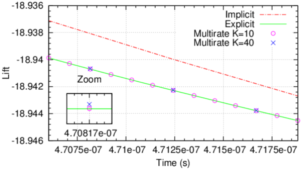

Figure 5: Left: Instantaneous pressure with streaklines; Right: Lift curves for explicit, implicit and multirate schemes.

K	CPU explicit (s/Δt/node)	$N^{small}(K)/N$ (%)	Expected gain (scalar)	CPU pred. phase (s/KΔt)	CPU cor. phase (s/KΔt)	Measured gain (parallel)	Error (%)
10	$4.13.10^{-7}$	0.015	8.69	1.81	4.36	2.93	1 10−5
40	$4.13.10^{-7}$	0.040	15.38	1.83	17.35	3.82	1.6 10−4
Implicit						36.88	$2\ .10^{-2}$

Table 7: **Spatial probe**: Time step factor K, CPU of the explicit scheme per explicit time-step Δt and per node, percentage of nodes in the inner region, theoretical gain in scalar mode, CPU of the prediction phase per time-step $K\Delta t$, CPU of the correction phase per time-step $K\Delta t$, measured parallel gain, and relative error.

Mesh partitioning improvement / Inner nodes

Mesh partitioning improvement / Inner nodes

- At the present time, domain decomposition designed to minimize the intercore communications (objective) under the requirement of an equivalent number of vertices in each partition (constraint)
  $\Longrightarrow$ inner nodes not equally distributed among the subdomains
  $\Longrightarrow$ loss of parallel efficiency due to a too costly correction phase
- Idea : multi-constraint partitioning (*) with weights assigned to vertices (the objective being always the minimization of the edge-cut)
  $\Longrightarrow$ two weights per node : a first weight equal for each node (first constraint : partitions of same size), a second weight more important for the inner nodes (second constraint : equal distribution of the inner nodes among the partitions)
  $\Longrightarrow$ a more efficient correction phase and multirate algorithm on parallel computers
- Use of Metis 5.1.0 software

(*) George Karypis and Vipin Kumar, *Multilevel Algorithms for Multi-Constraint Graph Partitioning*, Technical report # 98-019, university of Minnesota, 1998.

Conclusion, perspectives

- Presentation of a new **multirate scheme** based on agglomeration and relying on a **prediction step** and a **correction step**
- The proposed multirate strategy has been applied in **complex CFD problems** such as the prediction of three-dimensional flows around bluff bodies with complex hybrid turbulence models
- Progress is underway to **adapt the domain partitioning** in such a way that the cores workload becomes shared equally for both steps of the multirate scheme : use of weights in mesh partitioning (multi-constraint, Metis 5.1.0)
- Further efficiency can be gained in some cases if more than two zones can be considered (Inner zone - Medium zone - Outer Zone)
- Development in parallel of a **hybrid turbulence model** based on RANS and **VMS-LES** approaches with an **automatic RANS shielding zone**, applicable on a broad spectrum of Reynolds numbers and adapted to massive separated flows.

Thank you for your attention !

Appendix - Low Reynolds $k-\epsilon$ Goldberg Model

Modeling turbulent viscosity

Turbulent viscosity is modeled by : $\boxed{\mu_t = C_\mu f_\mu \rho \frac{k^2}{\epsilon}}$

where $C_\mu = 0.09$, and the **damping function** is given by : $f_\mu = \frac{1-e^{A_\mu R_t}}{1-e^{-R_t^{1/2}}} \max(1, \psi^{-1})$

with $A_\mu = 0.01, \psi = R_t^{1/2}/C_\tau, R_t = k^2/(\nu\varepsilon)$

Transport equations for low Reynolds $k-\epsilon$ Goldberg Model

The **turbulent kinetic energy** k and its **dissipation rate** ϵ, respectively, are determined by the following **transport equations**:

$$\frac{\partial \bar{\rho} k}{\partial t} + \frac{\partial(\bar{\rho}\tilde{v}_j k)}{\partial x_j} = \frac{\partial\left[\left(\mu + \frac{\mu_t}{\sigma_t}\right)\frac{\partial k}{\partial x_j}\right]}{\partial x_j} + \tau_{ij}\frac{\partial \tilde{v}_i}{\partial x_j} - \bar{\rho}\epsilon$$

and

$$\frac{\partial \bar{\rho}\epsilon}{\partial t} + \frac{\partial(\bar{\rho}\tilde{v}_j \epsilon)}{\partial x_j} = \frac{\partial\left[\left(\mu + \frac{\mu_t}{\sigma_\epsilon}\right)\frac{\partial \epsilon}{\partial x_j}\right]}{\partial x_j} + \left(C_{\epsilon 1}\tau_{ij}\frac{\partial \tilde{v}_i}{\partial x_j} - C_{\epsilon 2}\bar{\rho}\epsilon + E\right) T_\tau^{-1}$$

where $C_\tau = 1.41$, $C_{\epsilon 1} = 1.42$, $C_{\epsilon 2} = 1.83$, $E = \rho A_E V(\varepsilon T_\tau)^{0.5}\xi$ and the following realizable time scale is used here :

$$T_\tau = \frac{k}{\epsilon}\max(1, \psi^{-1})$$

with $A_E = 0.3$, $V = max(\sqrt{k},\ (\nu\varepsilon)^{0.25})$ and $\xi = max(\frac{\partial k}{\partial x_j}\frac{\partial \tau}{\partial x_j},\ 0)$ where $\tau = k/\varepsilon$.

Appendix

Menter correction

The **turbulent viscosity** is limited as follows :

$$\mu_t = \frac{\rho k \sqrt{C_\mu}}{max\left(\frac{\epsilon}{k\sqrt{C_\mu} f_\mu}, \mid r \mid \psi\right)}$$

where $\mid r \mid$ is the norm of the vorticity, $\psi = tanh(arg^2)$,

with $arg = max\left(2\frac{k^{3/2}}{\epsilon d}, \frac{500\nu B^* k}{d^2 \epsilon}\right)$, $\nu = \frac{\epsilon}{B^* k}$ and $B^* = 0.09 (= C_\mu)$